

www.acsanm.org Article

Carbonate-Terminated Self-Assembled Monolayers for Mimicking Nanoscale Polycarbonate Surfaces

Pooria Tajalli, Jennifer M. Hernandez Rivera, Mina Omidiyan, Hung-Vu Tran, and T. Randall Lee*



Cite This: ACS Appl. Nano Mater. 2023, 6, 2472–2477



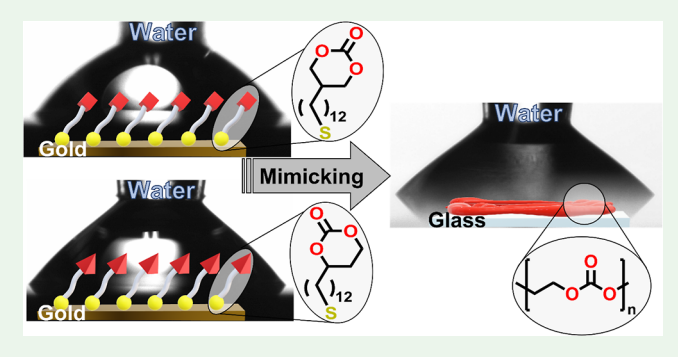
ACCESS

III Metrics & More

Article Recommendations

s Supporting Information

ABSTRACT: Two carbonate-terminated alkanethiol molecules having different positional isomers of a six-membered cyclic carbonate group, 3-COC12SH and 2-COC12SH, were synthesized and used to generate self-assembled monolayers (SAMs) on gold to serve as mimics of the surfaces of commercially available poly(propylene carbonate) (PPC) and poly(ethylene carbonate) (PEC). The adsorbate molecules were characterized using ¹H and ¹³C nuclear magnetic resonance spectroscopy and high-resolution mass spectrometry. The corresponding SAMs on gold were characterized by ellipsometry, contact angle goniometry, polarization-modulation infrared reflection-adsorption spectroscopy, and X-ray photoelectron spectroscopy. The contact angle data



showed that the wettabilities of both SAMs were largely similar to each other and to the PEC samples for a wide range of contacting probe liquids (with water correlating particularly well with PEC and both SAMs). As a whole, the wettability data suggest that the carbonate-terminated SAMs can serve as mimics of nanoscale polycarbonate surfaces and can be used to investigate the interfacial properties of polycarbonates without interference from the surface reconstruction.

KEYWORDS: carbonate-terminated, self-assembled monolayers (SAMs), polymer mimics, polycarbonates, poly(propylene carbonate) (PPC), poly(ethylene carbonate) (PEC), wettability, interfacial properties

■ INTRODUCTION

In 1962, Schnell et al. patented the first thermoplastic aromatic polycarbonates (PCs) and their manufacture based on the reaction of bisphenol A with phosgene. In 1969, Inoue et al. pioneered the synthesis of polycarbonates from carbon dioxide, one of the main greenhouse gases. Since then, PC materials have received considerable attention in various industries due to their toughness, light weight, optical transparency, and biocompatibility. In addition, the slow rates of biodegradation of PC materials to non-acidic products compared to other biocompatible polymers (e.g., polyesters, polylactides, and polycaprolactones) make them promising polymer coatings for bioactive materials and applications.

PC polymer chains can have either amorphous or crystalline morphologies. When amorphous, the polymer chains coil irregularly, and the polymer chains are parallel to each other when crystalline. Despite the stability of PC polymers, they tend to swell after being exposed to organic solvents. In polymer swelling, an organic solvent diffuses into the polymer matrix and allows polymer chains to reconstruct into their most favorable conformation, leading to the development of a crystalline structure. Consequently, polymer swelling induced by organic solvents leads to a change in the hydrophobicity of the polymer layers and makes it difficult

to study the interfacial properties of the polymer layers in contact with organic solvents. 12

Organic thin films have been widely used materials for modifying the interfacial properties of various surfaces. These nanoscale films, in the form of self-assembled monolayers (SAMs), have been utilized in various applications such as lubricants for microelectromechanical systems, ¹³ catalyst modifiers for hydrogenation reactions, ^{14,15} anti-corrosion protectants for metal surfaces, ^{16,17} and anti-adhesive films for surfaces and biosensors ^{18–20} due to their facile generation and manipulation. In further efforts to generate nanoscale films that mimic the surfaces of industrial polymers, ^{21,22} this paper describes the preparation of SAMs derived from the adsorption of alkanethiols terminated with 1,3-dioxane-2-one moieties on gold to serve as mimics to the surfaces of commercially available poly(propylene carbonate) (PPC) and poly(ethylene carbonate) (PEC). As shown in Figure 1, these 3-COC12SH and 2-COC12SH monolayers possess terminal carbonate

Received: October 31, 2022 Accepted: January 20, 2023 Published: February 6, 2023





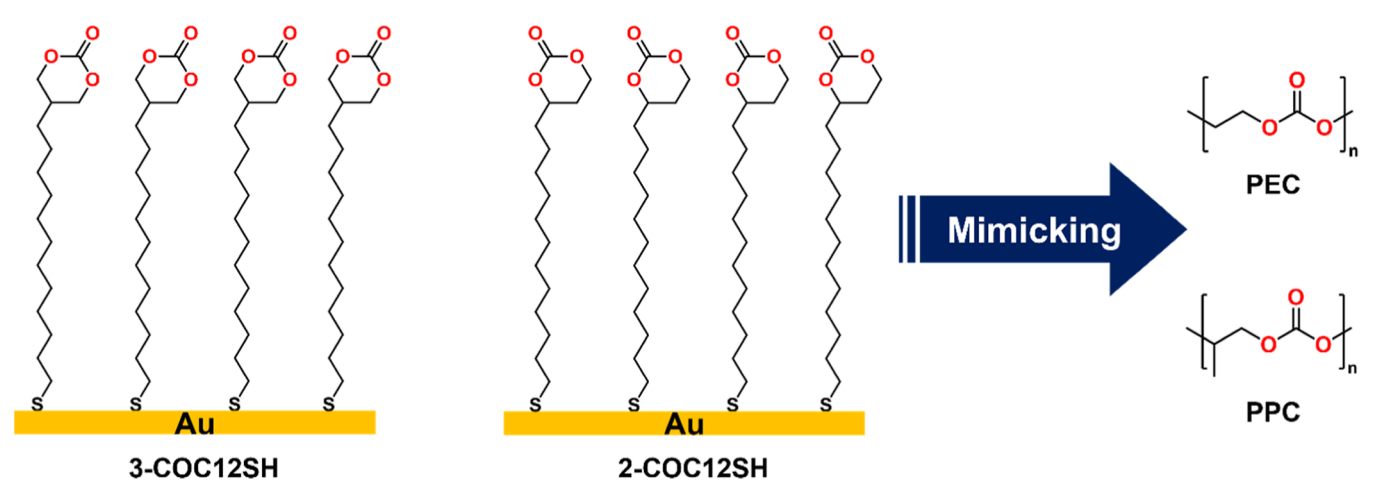


Figure 1. Molecular structures of the SAMs and polycarbonates examined in this study.

groups. Our hypothesis is based on the premise that SAMs derived from 3-COC12SH and 2-COC12SH would expose interfaces composed of the carbonate groups that can mimic the surfaces of polycarbonates but would not undergo surface reconstruction or swelling found in bulk polymer coatings. This study is part of a longstanding project to evaluate the damage that occurs to polymer coatings that undergo ion bombardment. Thus, we synthesized these two specific adsorbates having different positional isomers of the carbonate groups to generate SAMs and evaluate the interfacial characteristics of the carbonate groups, which are structurally similar to the backbones of PPC and PEC.

■ EXPERIMENTAL SECTION

Details of the materials, synthesis of the adsorbates, preparation of monolayers, procedures, and instrumental methods utilized in this manuscript are provided in the Supporting Information (presented graphically as Schemes S1 and S2 as well as Figures S1–S17).

RESULTS AND DISCUSSION

Ellipsometric Measurements. Monolayer films were characterized using ellipsometry after incubating gold slides in ethanolic solutions of the adsorbates for 24 h. ²⁵ Ellipsometry data are shown in Table 1. The thicknesses of SAMs generated

Table 1. Ellipsometric Thicknesses of SAMs Derived from C18SH and Carbonate Thiols

adsorbate	thickness (Å)
C18SH	19 ± 1
3-COC12SH	14 ± 1
2-COC12SH	16 ± 1

from well-known n-alkanethiols having comparable chain lengths (Table 1, row 1) can serve as references for our new SAMs. ²¹ With the ± 2 Å uncertainty in ellipsometric measurements, the thickness of our reference C18SH SAMs is within the experimental error of the literature values; ^{21,26} notably, these values can vary with the quality and cleanliness of the evaporated gold substrates. Comparison between carbonate-terminated monolayers and their analogous n-alkanethiols SAMs possessing a similar number of atoms in their alkyl chain revealed that the 3-COC12SH and 2-COC12SH monolayers were thinner than the analogous n-alkanethiols SAMs, which can be attributed to the bulkiness of the six-membered rings on

the 3-COC12SH and 2-COC12SH adsorbate molecules and the consequent decrease in molecular packing density on the gold surface. We note also that the thickness of the 2-COC12SH SAMs (16 Å) is within experimental error of the thickness of the 3-COC12SH SAMs (14 Å), which is consistent with the polarization-modulation infrared reflection-adsorption spectroscopy (PM-IRRAS) data for the films (vide infra).

X-ray Photoelectron Spectroscopy Analysis of the Films. X-ray photoelectron spectroscopy (XPS) is a surface-sensitive technique that provides reliable quantitative analyses of the elemental composition of surfaces. In XPS, the binding energy (BE) of the emitted photoelectrons of individual atoms is detected, and each atom produces a unique set of characteristic XPS peaks in which the chemical environment of atoms, as well as their oxidation state, can be determined. The XPS spectra of the S 2p, C 1s, and O 1s regions of the studied monolayers are shown in Figure 3 and referenced to the Au $4f_{7/2}$ peak at 84 eV.

As shown in Figure 2A, the spin-orbit-split doublet for bound thiol appears at ~162 and ~163 eV, in a 2:1 ratio, assigned to S $2p_{3/2}$ and S $2p_{1/2}$, respectively. ^{26,28,29} On the other hand, the BE of unbound thiol groups and highly oxidized sulfur species have been reported to have spin-orbitsplit S 2p peaks centered at ~164 and ~166 eV, respectively.²² The absence of both ~164 and ~166 eV peaks in Figure 2A indicates that SAMs derived from n-alkanethiols and carbonate-terminated thiols in this study have no significant unbound or oxidized sulfur species. 26,28 The peak position of the C 1s region for the CH₃/CH₂ unit in C18SH, 3-COC12SH, and 2-COC12SH SAMs appears at ~284.8 eV (Figure 2B). Moreover, the XPS spectra show two more peaks for 3-COC12SH and 2-COC12SH with the BEs of ~286.8 eV for C-O and ~290.6 eV for C=O species, confirming the presence of carbonate groups in the monolayers. 30,31 In Figure 2C, the peak positions of the O 1s region for C=O and C-O are shown with BEs of ~532.4 and ~533.8 eV, respectively.³²

The relative packing density of SAMs can be determined by calculating the ratio of the integrated areas of peaks in the S 2p region to the integrated area of peaks in the Au 4f region and normalizing the adsorbate packing density to be 100% for the C18SH SAMs. 21 As shown in Table 2, the BEs of the S $2p_{3/2}$ and C 1s bands are within the experimental error for all three SAMs. Both of the SAMs derived from 3-COC12SH and 2-COC12SH, which are different structural isomers of

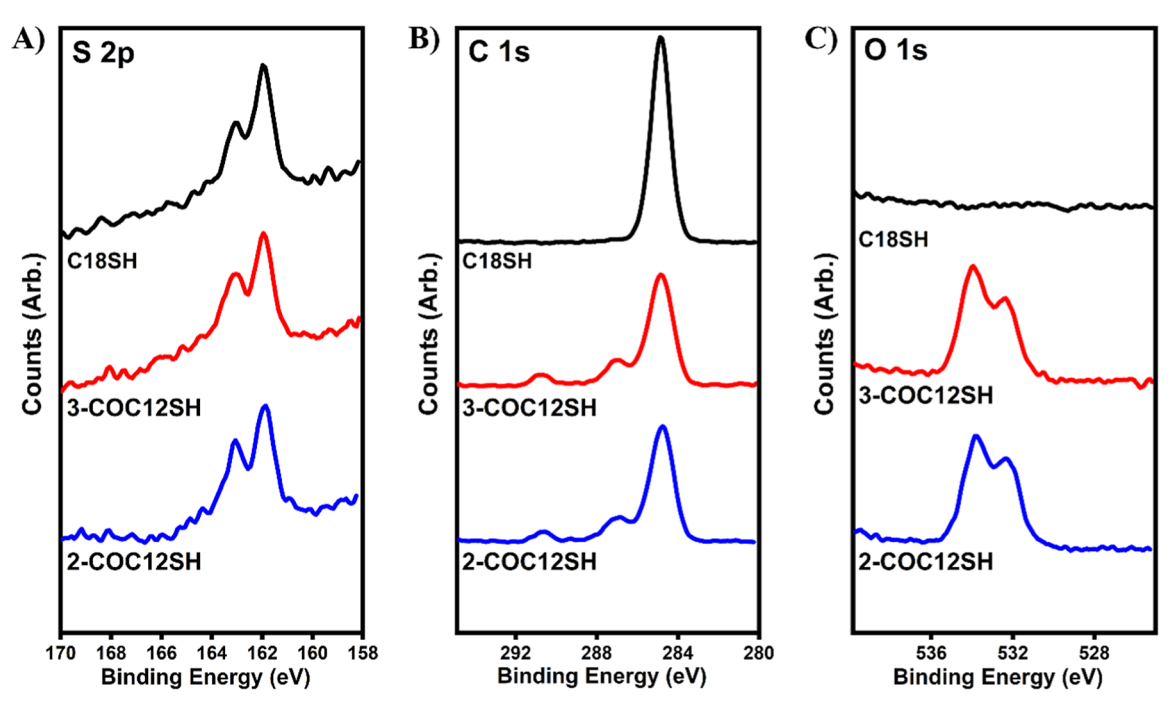


Figure 2. XPS spectra for the (A) S 2p, (B) C 1s, and (C) O 1s of the C18SH, 3-COC12SH, and 2-COC12SH SAMs.

Table 2. Binding Energies and Relative Packing Densities of the SAMs Derived from C18SH, 3-COC12SH, and 2-COC12SH

adsorbate	S 2p _{3/2} (eV)	C 1s (CH ₂) (eV)	C 1s (C-O) (eV)	C 1s (C=O) (eV)	O 1s (C-O) (eV)	O 1s (C=O) (eV)	relative packing density (%)
C18SH	161.9	284.8					100
3-COC12SH	161.9	284.8	286.9	290.6	533.9	532.4	94 ± 4
2-COC12SH	161.8	284.7	286.8	290.5	533.8	532.4	95 ± 3

carbonate-terminated thiols, showed relatively high packing densities of 94 and 95%, respectively. Further evidence of high packing density for both carbonate-terminated SAMs was provided by the C 1s binding energies, which are indistinguishable from the C 1s binding energies of the densely-packed SAMs derived from C18SH. Notably, densely packed films act as better insulators than loosely packed films, preventing positive charges generated by photoelectron emission from being discharged and thereby giving rise to high C 1s binding energies.³³

PM-IRRAS Analysis of the Films. Polarization modulation infrared reflection-adsorption spectroscopy (PM-IRRAS) has been used to explore structural information of SAMs such as chain orientation and conformational order.³⁴ Specifically, the conformational order or "crystallinity" of the alkyl chains can be evaluated by the peak position of the antisymmetric methylene C–H stretching vibration (ν_a^{CH}₂).³⁴ For highly crystalline films, this band appears at ~2918 cm⁻¹, indicating well-ordered alkyl chains that are predominantly trans-extended; the presence of gauche defects in the alkyl chains causes this band to blue-shift to higher wavenumbers.^{35,36} PM-IRRAS spectra of the C–H stretching region for the SAMs generated from **C18SH** and the carbonate-terminated monolayers are shown in Figure 3 and are tabulated in Table 3.

Table 3 provides the peak positions and assignments of the C-H stretching region for the studied SAMs. The 3-COC12SH and 2-COC12SH SAMs display a $\nu_{as}^{CH_2}$ band at \sim 2920 cm⁻¹ indicating a well-ordered monolayer and having

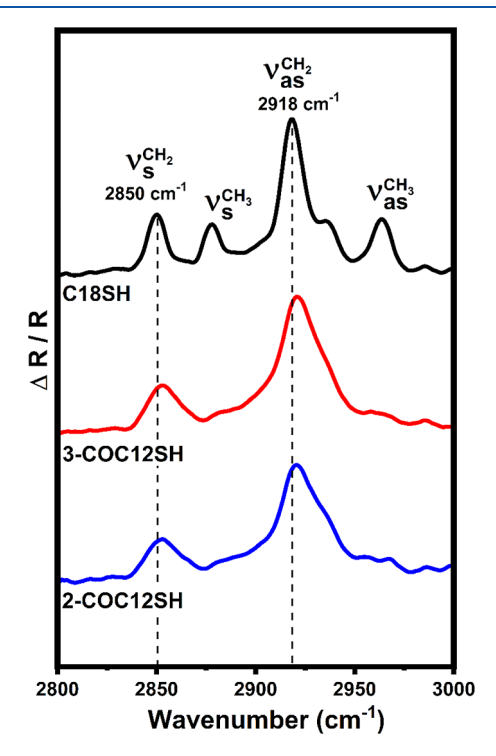


Figure 3. PM-IRRAS spectra of the C-H stretching region for SAMs derived from C18SH, 3-COC12SH, and 2-COC12SH.

largely trans-extended alkyl chains since the peak position is close to the $v_{as}^{CH_2}$ band of the trans-extended alkyl chains of

Table 3. PM-IRRAS Data for SAMs Generated from C18SH, 3-COC12SH, and 2-COC12SH

adsorbate	$v_{\rm s}^{\rm CH_2}$ $({\rm cm}^{-1})$	$(cm^{CH_3}$	$(\mathrm{cm}^{\mathrm{CH_2}})$	(cm^{CH_3})
C18SH	2850	2878	2918	2964
3-COC12SH	2853		2920	
2-COC12SH	2853		2920	

C18SH at ~2918 cm⁻¹. 35,36 Interestingly, monolayers bearing the terminal carbonate groups studied here showed greater conformational order than cyclohexyl-terminated films having the same chain length for which the $\nu_{as}^{CH_2}$ band appears at ~2924 cm^{-1,21} This phenomenon is consistent with the observations above obtained from ellipsometric thickness measurements and XPS (vide supra). It is possible that the greater conformational order for the carbonate-terminated SAMs arises from favorable dipole-dipole interactions of the carbonate groups compared to the weaker van der Waals interactions of the cyclohexyl groups in the cyclohexylterminated SAMs reported previously.

Wettability of the Films. The wettability of carbonateterminated SAMs and their counterparts (PPC and PEC) were examined using various types of probe liquids including polar protic solvents such as water (W, $\gamma_{LV} = 72.8 \text{ mN/m}$, $\gamma_{LV}^p =$ 51.0 mN/m, γ_{LV}^{d} = 21.8 mN/m), glycerol (Gly, γ_{LV} = 64.0 mN/m), formamide (FA, γ_{LV} = 58.2 mN/m), and Nmethylformamide (MF, $\gamma_{LV} = 38.0 \text{ mN/m}$); polar aprotic solvents such as dimethyl sulfoxide (DMSO, γ_{LV} = 43.7 mN/ m), N,N-dimethylformamide (DMF, $\gamma_{LV} = 37.1$ mN/m), and acetonitrile (MeCN, γ_{LV} = 29.1 mN/m); and apolar aprotic solvents such as dijodomethane (DIM, γ_{LV} = 50.8 mN/m, γ_{LV}^{p} = 0.0 mN/m, γ_{LV}^{d} = 50.8 mN/m), decalin (DC, γ_{LV} = 31.5 mN/m), squalane (SQ, $\gamma_{LV} = 28.9$ mN/m), and hexadecane (HD, $\gamma_{LV} = 27.5$ mN/m). Table 4 lists the advancing contact angles and the hysteresis values, which correspond to the difference between the advancing and receding contact angles for all probe liquids on the surfaces of the polymers PEC and PPC as well as the SAMs derived from 3-COC12SH and 2-COC12SH. The corresponding optical images of the advancing contact angles are provided in Figures \$7-\$17 in the Supporting Information. Importantly, the surfaces of PEC and PPC became swollen (and likely reconstructed) when contacted with MF, DMSO, DMF, and MeCN; notably, the carbonate-terminated SAM surfaces also interacted strongly with these probe liquids due to polar interactions and were completely wet by them. The probe liquids having low surface tensions (i.e., DC, SQ, and HD) also wet the surfaces as expected.40,41

Limiting our further discussion to the probe liquids where measurable contact angles were observed, Figure 4 shows the

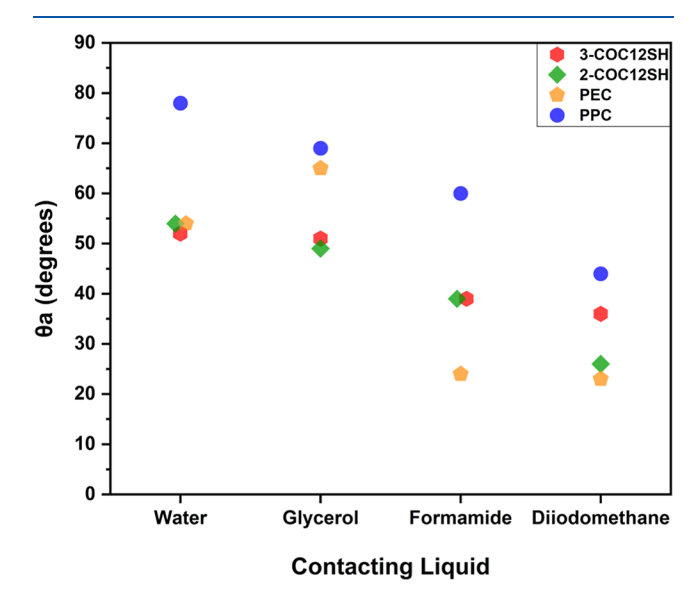


Figure 4. Advancing contact angle values obtained on the carbonateterminated SAMs and the corresponding polycarbonates. Error bars, which are not visible, fall within the symbols. Contact angles having identical values are slightly offset horizontally for clarity.

advancing contact angle values for water, formamide, glycerol, and diiodomethane on the studied surfaces. The contact angles of water were the same for the 3-COC12SH and 2-COC12SH SAMs (\sim 52 to 54°), indicating a similar interaction with water for both of these films (e.g., due to hydrogen bonding). The advancing contact angle values for formamide and glycerol were also roughly the same on the 3-COC12SH and 2-COC12SH SAMs, and the only notable differences were observed for diiodomethane whose large steric bulk prohibits intercalation into the films. 42 Comparison of the wettabilities of the SAMs with that of the polymers (see Figure 4) found that the wettabilities of the SAMs toward the polar protic probe liquids W, Gly, and FA are more comparable to PEC than to PPC, particularly for water. This trend can be rationalized by the presence of the methyl group in each repeat unit of PPC, which makes this polymer more hydrophobic than PEC and thereby diminishes its wettability toward the polar protic probe liquids.

Interestingly, the contact angles on the carbonate SAMs and polymer surfaces of the polar protic probe liquids, when ordered based on their surface tensions (from highest to lowest) in Table 4, showed a decreasing trend in value when

Table 4. Advancing Contact Angles of the Investigated SAMs and Polymers Using Various Probe Liquids

	polar protic solvents			polar aprotic solvents			non-polar solvents				
adsorbate	W	Gly	FA	MF	DMSO	DMF	MeCN	DIM	DC	SQ	HD
3-COC12SH	52 (9)	51 (13)	39 (5)	<10 (-)	<10 (-)	<10 (-)	<10 (-)	36 (7)	<10 (-)	<10 (-)	<10 (-)
2-COC12SH	54 (8)	49 (12)	39 (6)	<10 (-)	<10 (-)	<10 (-)	<10 (-)	26 (6)	<10 (-)	<10 (-)	<10 (-)
PEC	54 (11)	65 (12)	24 (5)	X^a	X^a	X^a	X^a	23 (6)	<10 (-)	<10 (-)	<10 (-)
PPC	78 (15)	69 (8)	60 (12)	X^a	X^a	X^a	X^a	44 (8)	<10 (-)	<10 (-)	<10 (-)

^aContact angle measurement was not possible due to the change in polymer structures caused by interaction with the liquid. Values of hysteresis are given in parentheses. Water (W), glycerol (Gly), formamide (FA), N-methylformamide (MF), dimethyl sulfoxide (DMSO), N,Ndimethylformamide (DMF), acetonitrile (MeCN), diiodomethane (DIM), decalin (DC), squalane (SQ), hexadecane (HD), poly(ethylene carbonate) (PEC), and poly(propylene carbonate) (PPC).

the surface tension decreased. This trend can be rationalized by the decrease in surface tension of these probe liquids caused by systematically decreasing the intermolecular forces within the liquids, leading to stronger interactions with the surfaces (i.e., increasing wettability). Further, the advancing contact angles of the polar protic liquids are consistent with a model in which the polar probe liquids interact favorably with the carbonate terminal groups of the 3-COC12SH and 2-COC12SH SAMs.

Similarly, decalin, squalene, and hexadecane, the apolar aprotic liquids with lower surface tensions than diiodomethane, fully wet all monolayer and polymer surfaces due to the strong van der Waals interactions between the probe liquids and the methylene groups in the SAMs and in the polymers. Finally, the hysteresis data, which provide insight into the roughness and/or heterogeneity (e.g., surface reconstruction) of the surfaces, 40,43 showed similar values for all surfaces for which reliable advancing and receding contact angles could be measured.

CONCLUSIONS

Two carbonate-terminated thiol adsorbates 3-COC12SH and 2-COC12SH were designed, synthesized, and used to generate nanoscale monolayers on gold substrates. From PM-IRRAS analysis, the C-H antisymmetric stretching vibration of the alkyl spacer of the SAMs showed that the 3-COC12SH and 2-COC12SH SAMs adopted an all trans-extended conformation. The packing densities of the monolayers were calculated by the integrated area of S/Au in XPS measurements. The results showed that both SAMs have high packing densities and are conformationally ordered. Importantly, the contact angle data showed that the wettability of both 3-COC12SH and 2-COC12SH SAMs was largely similar to each other and to the PEC samples for a wide range of contacting probe liquids (with water correlating particularly well with PEC and both SAMs). Consequently, the SAMs studied here can serve as mimics of nanoscale polycarbonate surfaces and can be used to investigate the interfacial properties of polycarbonates in the absence of swelling and/or surface reconstruction.

ASSOCIATED CONTENT

Supporting Information

The Supporting Information is available free of charge at https://pubs.acs.org/doi/10.1021/acsanm.2c04742.

Details of the materials utilized, adsorbate synthesis, adsorbate characterization, SAM characterization, and experimental methods including polymer spin-coating procedures (PDF)

AUTHOR INFORMATION

Corresponding Author

T. Randall Lee – Department of Chemistry and the Texas Center for Superconductivity, University of Houston, Houston, Texas 77204-5003, United States; orcid.org/0000-0001-9584-8861; Email: trlee@uh.edu

Authors

Pooria Tajalli – Department of Chemistry and the Texas Center for Superconductivity, University of Houston, Houston, Texas 77204-5003, United States; orcid.org/ 0000-0001-7415-0587

- Jennifer M. Hernandez Rivera Department of Chemistry and the Texas Center for Superconductivity, University of Houston, Houston, Texas 77204-5003, United States;

 orcid.org/0000-0001-8298-6288
- Mina Omidiyan Department of Chemistry and the Texas Center for Superconductivity, University of Houston, Houston, Texas 77204-5003, United States; orcid.org/ 0000-0002-5017-5269
- Hung-Vu Tran Department of Chemistry and the Texas Center for Superconductivity, University of Houston, Houston, Texas 77204-5003, United States; ⊙ orcid.org/ 0000-0001-8536-2737

Complete contact information is available at: https://pubs.acs.org/10.1021/acsanm.2c04742

Notes

The authors declare no competing financial interest.

ACKNOWLEDGMENTS

The authors appreciate the financial support received from the National Science Foundation (CHE-2109174) and the Robert A. Welch Foundation (grant no. E-1320).

REFERENCES

- (1) Hermann, S.; Ludwig, B.; Heinrich, K. Thermoplastic Aromatic Polycarbonates and Their Manufacture. U.S. Patent 3,028,365 A, 1962
- (2) Inoue, S.; Koinuma, H.; Tsuruta, T. Copolymerization of Carbon Dioxide and Epoxide with Organometallic Compounds. *Makromol. Chem.* **1969**, *130*, 210–220.
- (3) Wang, P.; Park, J. H.; Sayed, M.; Chang, T.-S.; Moran, A.; Chen, S.; Pyo, S.-H. Sustainable Synthesis and Characterization of a Bisphenol A-Free Polycarbonate from a Six-Membered Dicyclic Carbonate. *Polym. Chem.* **2018**, *9*, 3798–3807.
- (4) Montagna, V.; Takahashi, J.; Tsai, M.-Y.; Ota, T.; Zivic, N.; Kawaguchi, S.; Kato, T.; Tanaka, M.; Sardon, H.; Fukushima, K. Methoxy-Functionalized Glycerol-Based Aliphatic Polycarbonate: Organocatalytic Synthesis, Blood Compatibility, and Hydrolytic Property. ACS Biomater. Sci. Eng. 2021, 7, 472–481.
- (5) Anju, S.; Prajitha, N.; Sukanya, V. S.; Mohanan, P. V. Complicity of Degradable Polymers in Health-Care Applications. *Mater. Today Chem.* **2020**, *16*, 100236.
- (6) Mohajeri, S.; Amsden, B. G. In Vivo Degradation Mechanism and Biocompatibility of a Biodegradable Aliphatic Polycarbonate: Poly(trimethylene carbonate-co-5-hydroxy trimethylene carbonate). ACS Appl. Bio Mater. 2021, 4, 3686–3696.
- (7) Kong, D.-C.; Yang, M.-H.; Zhang, X.-S.; Du, Z.-C.; Fu, Q.; Gao, X.-Q.; Gong, J.-W. Control of Polymer Properties by Entanglement: A Review. *Macromol. Mater. Eng.* **2021**, *306*, 2100536.
- (8) Ong, C. S.; Lay, H. T.; Tamilselvam, N. R.; Chew, J. W. Cross-Linked Polycarbonate Microfiltration Membranes with Improved Solvent Resistance. *Langmuir* **2021**, *37*, 4025–4032.
- (9) Ogieglo, W.; Ghanem, B.; Ma, X.; Pinnau, I.; Wessling, M. How Much Do Ultrathin Polymers with Intrinsic Microporosity Swell in Liquids? *J. Phys. Chem. B* **2016**, *120*, 10403–10410.
- (10) Gugliuzza, A. Solvent Swollen Polymer. In *Encyclopedia of Membranes*; Drioli, E., Giorno, L., Eds.; Springer Berlin Heidelberg: Berlin, Heidelberg, 2016; pp 1801–1802.
- (11) Zaleski, R.; Krasucka, P.; Skrzypiec, K.; Goworek, J. Macro- and Nanoscopic Studies of Porous Polymer Swelling. *Macromolecules* **2017**, *50*, 5080–5089.
- (12) Wang, J.; Klok, H.-A. Swelling-Induced Chain Stretching Enhances Hydrolytic Degrafting of Hydrophobic Polymer Brushes in Organic Media. *Angew. Chem., Int. Ed.* **2019**, *58*, 9989–9993.
- (13) Cooper, O.; Phan, H.-P.; Wang, B.; Lowe, S.; Day, C. J.; Nguyen, N.-T.; Tiralongo, J. Functional Microarray Platform with

- Self-Assembled Monolayers on 3C-Silicon Carbide. *Langmuir* **2020**, 36, 13181–13192.
- (14) Kahsar, K. R.; Schwartz, D. K.; Medlin, J. W. Control of Metal Catalyst Selectivity through Specific Noncovalent Molecular Interactions. *J. Am. Chem. Soc.* **2014**, *136*, 520–526.
- (15) Coan, P. D.; Farberow, C. A.; Griffin, M. B.; Medlin, J. W. Organic Modifiers Promote Furfuryl Alcohol Ring Hydrogenation via Surface Hydrogen-Bonding Interactions. ACS Catal. 2021, 11, 3730—3739.
- (16) Sui, W.; Zhao, W.; Zhang, X.; Peng, S.; Zeng, Z.; Xue, Q. Comparative Anti-Corrosion Properties of Alkylthiols SAMs and Mercapto Functional Silica Sol—Gel Coatings on Copper Surface in Sodium Chloride Solution. *J. Sol-Gel Sci. Technol.* **2016**, *80*, 567–578.
- (17) Telegdi, J. Formation of Self-Assembled Anticorrosion Films on Different Metals. *Materials* **2020**, *13*, 5089.
- (18) Choi, Y.; Tran, H.-V.; Lee, T. R. Self-Assembled Monolayer Coatings on Gold and Silica Surfaces for Antifouling Applications: A Review. *Coatings* **2022**, *12*, 1462.
- (19) St. Hill, L. R.; Craft, J. W.; Chinwangso, P.; Tran, H.-V.; Marquez, M. D.; Lee, T. R. Antifouling Coatings Generated from Unsymmetrical Partially Fluorinated Spiroalkanedithiols. *ACS Appl. Bio Mater.* **2021**, *4*, 1563–1572.
- (20) St. Hill, L. R.; Tran, H.-V.; Chinwangso, P.; Lee, H. J.; Marquez, M. D.; Craft, J. W.; Lee, T. R. Antifouling Studies of Unsymmetrical Oligo(ethylene glycol) Spiroalkanedithiol Self-Assembled Monolayers. *Micro* **2021**, *1*, 151–163.
- (21) Barriet, D.; Chinwangso, P.; Lee, T. R. Can Cyclopropyl-Terminated Self-Assembled Monolayers on Gold Be Used to Mimic the Surface of Polyethylene? *ACS Appl. Mater. Interfaces* **2010**, *2*, 1254–1265.
- (22) Yu, T.; Marquez, M. D.; Zenasni, O.; Lee, T. R. Mimicking Polymer Surfaces Using Cyclohexyl- and Perfluorocyclohexyl-Terminated Self-Assembled Monolayers. *ACS Appl. Nano Mater.* **2019**, 2, 5809–5816.
- (23) Smith, D. L.; Wysocki, V. H.; Colorado, R., Jr.; Shmakova, O. E.; Graupe, M.; Lee, T. R. Low-Energy Ion-Surface Collisions Characterize Alkyl- and Fluoroalkyl-Terminated Self-Assembled Monolayers on Gold. *Langmuir* **2002**, *18*, 3895–3902.
- (24) Somogyi, Á.; Smith, D. L.; Wysocki, V. H.; Colorado, R., Jr.; Lee, T. R. Neutralization of Methyl Cation via Concerted Chemical Reactions in Low-Energy Ion-Surface Collisions. *J. Am. Soc. Mass Spectrom.* **2002**, *13*, 1151–1161.
- (25) Rodriguez, D.; Marquez, M. D.; Zenasni, O.; Han, L. T.; Baldelli, S.; Lee, T. R. Surface Dipoles Induce Uniform Orientation in Contacting Polar Liquids. *Chem. Mater.* **2020**, *32*, 7832–7841.
- (26) Bain, C. D.; Troughton, E. B.; Tao, Y. T.; Evall, J.; Whitesides, G. M.; Nuzzo, R. G. Formation of Monolayer Films by the Spontaneous Assembly of Organic Thiols from Solution onto Gold. *J. Am. Chem. Soc.* **1989**, *111*, 321–335.
- (27) Choi, Y.; Park, C. S.; Tran, H.-V.; Li, C.-H.; Crudden, C. M.; Lee, T. R. Functionalized *N*-Heterocyclic Carbene Monolayers on Gold for Surface-Initiated Polymerizations. *ACS Appl. Mater. Interfaces* **2022**, *14*, 44969–44980.
- (28) Castner, D. G.; Hinds, K.; Grainger, D. W. X-Ray Photoelectron Spectroscopy Sulfur 2p Study of Organic Thiol and Disulfide Binding Interactions with Gold Surfaces. *Langmuir* **1996**, *12*, 5083— 5086
- (29) Yu, T.; Marquez, M. D.; Tran, H.-V.; Lee, T. R. Crosslinked Organosulfur-Based Self-Assembled Monolayers: Formation and Applications. *Soft Sci.* **2022**, *2*, 5.
- (30) Chen, X.; Wang, X.; Fang, D. A Review on C1s XPS-Spectra for Some Kinds of Carbon Materials. *Fuller. Nanotub.* **2020**, 28, 1048–1058.
- (31) Oswald, S.; Thoss, F.; Zier, M.; Hoffmann, M.; Jaumann, T.; Herklotz, M.; Nikolowski, K.; Scheiba, F.; Kohl, M.; Giebeler, L.; Mikhailova, D.; Ehrenberg, H. Binding Energy Referencing for XPS in Alkali Metal-Based Battery Materials Research (II): Application to Complex Composite Electrodes. *Batteries* **2018**, *4*, 36.

- (32) Marandi, A.; Kolvari, E.; Gilandoust, M.; Zolfigol, M. A. Immobilization of –OSO₃H on Activated Carbon Powder and Its Use as a Heterogeneous Catalyst in the Synthesis of Phthalazine and Quinoline Derivatives. *Diam. Relat. Mater.* **2022**, *124*, 108908.
- (33) Ishida, T.; Hara, M.; Kojima, I.; Tsuneda, S.; Nishida, N.; Sasabe, H.; Knoll, W. High Resolution X-Ray Photoelectron Spectroscopy Measurements of Octadecanethiol Self-Assembled Monolayers on Au(111). *Langmuir* 1998, 14, 2092–2096.
- (34) Porter, M. D.; Bright, T. B.; Allara, D. L.; Chidsey, C. E. D. Spontaneously Organized Molecular Assemblies. 4. Structural Characterization of *n*-Alkyl Thiol Monolayers on Gold by Optical Ellipsometry, Infrared Spectroscopy, and Electrochemistry. *J. Am. Chem. Soc.* **1987**, *109*, 3559–3568.
- (35) MacPhail, R. A.; Strauss, H. L.; Snyder, R. G.; Elliger, C. A. Carbon-Hydrogen Stretching Modes and the Structure of *n*-Alkyl Chains. 2. Long, All-Trans Chains. *J. Phys. Chem.* **1984**, *88*, 334–341.
- (36) Snyder, R. G.; Strauss, H. L.; Elliger, C. A. Carbon-Hydrogen Stretching Modes and the Structure of *n*-Alkyl Chains. 1. Long, Disordered Chains. *J. Phys. Chem.* **1982**, *86*, 5145–5150.
- (37) Smallwood, I. Handbook of Organic Solvent Properties; Butterworth-Heinemann: Woburn, MA, 2014.
- (38) Wohlfarth, C. Surface Tension of Pure Liquids and Binary Liquid Mixtures, 2008th ed.; Lechner, M. D., Ed.; Landolt-Börnstein: Numerical Data and Functional Relationships in Science and Technology-New Series; Springer: Berlin, Germany, 2008.
- (39) Wu, W.; Giese, R. F., Jr.; van Oss, C. J. Evaluation of the Lifshitz-van Der Waals/Acid-Base Approach To Determine Surface Tension Components. *Langmuir* 1995, 11, 379–382.
- (40) Lee, S.; Park, J.-S.; Lee, T. R. The Wettability of Fluoropolymer Surfaces: Influence of Surface Dipoles. *Langmuir* **2008**, *24*, 4817–4826.
- (41) Yuan, Y.; Lee, T. R. Contact Angle and Wetting Properties. *Surface Science Techniques*; Bracco, G., Holst, B., Eds.; Springer Berlin Heidelberg: Berlin, Heidelberg, 2013; pp 3–34.
- (42) Yu, T.; Marquez, M. D.; Lee, T. R. SAMs on Gold Derived from Adsorbates Having Phenyl and Cyclohexyl Tail Groups Mixed with Their Phase-Incompatible Fluorinated Analogues. *Langmuir* **2022**, *38*, 13488–13496.
- (43) Wang, J.; Wu, Y.; Cao, Y.; Li, G.; Liao, Y. Influence of Surface Roughness on Contact Angle Hysteresis and Spreading Work. *Colloid Polym. Sci.* **2020**, 298, 1107–1112.